Peak Power Analysis of MC-CDMA Employing Golay Complementary Sequences

Lin Dong

A thesis presented to Lakehead University

in partial fulfillment of the requirement for the degree of

Master of Science in Electrical and Computer Engineering

Thunder bay, Ontario, Canada

May 5, 2011

Abstract

Multicarrier code division multiple access (MC-CDMA) combines both orthogonal frequency division multiplexing (OFDM) and code division multiple access (CDMA) techniques. It inherits the advantages of these two techniques. However, like the OFDM system, transmitted signal of MC-CDMA system suffers from the high peak-to-average power ratio (PAPR) as well.

As a good solution to reduce the high peak-to-average power ratio (PAPR), Golay complementary sequences have been employed in multicarrier communication systems. In this thesis, we present a simple but novel technique to analyse the theoretical PAPR bounds of downlink MC-CDMA system using Golay complementary sequences for spreading and/or coding. We first develop the PAPR bounds of uncoded MC-CDMA system using binary Golay complementary spreading sequences. Then, we develop the PAPR bounds when each user's transmitted data is encoded as QPSK Golay sequences or 16-QAM Golay sequences. Simulation results demonstrate that the theoretical PAPR bounds and 99.9% PAPRs are independent of the spreading factor for uncoded case. For coded case, the theoretical PAPR bounds and 99.9% PAPRs are independent of the number of spreading processes as well as the spreading factor. Practically, the independency shows that Golay complementary sequences are useful for peak power control in downlink MC-CDMA system.

Contents

List of Figures

List of Tables

Chapter 1

Introduction

1.1 Multicarrier CDMA

Multicarrier CDMA (MC-CDMA) is a hybrid modulation scheme based on OFDM and CDMA techniques. It was first proposed by Yee, Linnartz and Fettweis [1], Chouly, Brajal and Jourdan [2], and Fettweis, Bahai and Anvari [3]. As a combination scheme, it joints the advantages of both OFDM and CDMA, such as high spectrum efficiency, frequency diversity, immunity to multipath fading and impulse noise, etc. Additionally, due to its low complexity, multicarrier CDMA systems have been broadly proposed in broadband wireless multimedia applications.

However, due to the same transmitter structure as the OFDM system, MC-CDMA also suffers from the high peak-to-average power ratio (PAPR) [4]. For multicarrier communications, PAPR mainly

depends on the number of subcarriers. The higher the number of subcarriers, the higher the PAPR will be. The high PAPR brings disadvantages such as an increased complexity of the analog-to-digital (A/D) and digital-to-analog (D/A) converters and a reduced efficiency of the power amplifier. These disadvantages can put a high requirement on transmitter and receiver design [5, 6]. Thus, in most low cost applications, the high PAPR may outweigh all the possible advantages of multicarrier communication systems [7].

1.2 Motivation

To date, a variety of techniques have been studied in MC-CDMA systems to solve the high PAPR problem [8]-[13]. Among them, optimizing the spreading sequences is a direct and effective way to reduce the high PAPR of MC-CDMA systems [14, 15, 16]. In [14], through examining various sequences, such as Walsh [17], Gold [18], Orthogonal Gold [19], Zadoff-Chu sequences [20], Legendre [21] and Golay complementary sequences [22], the basic criteria of selecting the code sets for both PAPR and the dynamic range reduction has been established. In [15], the authors achieve the PAPR reduction by dynamically changing the spreading sequences between Walsh Hardamard spreading sequences and Golay complementary spreading sequences. In [16], the authors provide a reduced search algo-

rithm to find the optimum Walsh-Hadamard code sets to minimize the PAPR. However, until now, the PAPR properties of MC-CDMA system are studied mostly through experiments. These experiments are seldomly backed up by theoretical PAPR analysis of MC-CDMA signals. For this reason, we devote our efforts in this thesis to theoretical analysis of the PAPR properties of the MC-CDMA system.

Among the sequences studied so far, we choose Golay complementary sequences as the spreading and/or coding to analyze the theoretical PAPR properties of downlink MC-CDMA system. Golay complementary sequences [22] have been widely studied and employed in multicarrier communication systems due to their bounded PAPR [23]. At the same time, as the spreading sequences in MC-CDMA system, Golay complementary sequences are known for their stable PAPR property. Compared to Walsh-Hadamard sequences, MC-CDMA system using Golay complementary spreading sequences can support various numbers of active users without dramatic PAPR fluctuation [15].

1.3 Contributions

In this thesis, we first develop the theoretical PAPR bounds of uncoded downlink MC-CDMA system using Golay complementary sequences only for spreading. We adopt both M-PSK and M-QAM

modulation schemes to analyse the theoretical PAPR bounds of downlink MC-CDMA system where binary Golay complementary sequences are employed for spreading.

Furthermore, we develop the theoretical PAPR bounds of the coded downlink MC-CDMA system where either QPSK or 16-QAM Golay complementary sequences [24, 25] are empolyed as the codewords input to binary Golay spreading sequences. To support L users, L different Golay complementary sequences of length N are chosen as orthogonal spreading sequences, where each of $\lfloor \frac{L}{2} \rfloor$ pairs forms a Golay complementary pair.

We find that the theoretical PAPR bounds are independent of the spreading factor N in uncoded case. For coded case, the theoretical PAPR bounds are independent of both the spreading factor N and the number of spreading processes K. As a result, the PAPR bounds of coded MC-CDMA depend on the number of active users L only from which we equivalently achieve dramatic PAPR reduction compared to uncoded MC-CDMA.

Finally, we numerically demonstrate through simulation results that both the developed theoretical PAPR bounds and numerical 99.9% PAPRs are independent of the spreading factor N for uncoded case. For coded case, the theoretical PAPR bounds and 99.9% PAPRs are independent of the number of spreading processes K as well as the spreading factor N. From the independency of coded case, we can significantly reduce the PAPR of coded MC-CDMA with a

large number of subcarriers. The independency shows that Golay complementary sequences are a useful way for peak power control in downlink MC-CDMA system.

Thesis outline

The remainder of this thesis is structured as follows. Chapter 2 introduces the background concepts used in this thesis, such as M-PSK, M-QAM, OFDM, spread spectrum technologies, MC-CDMA and PAPR. Chapter 3 gives the direct construction method of Golay complementary sequences for spreading and/or coding purpose. Chapter 4 mathematically describes the downlink MC-CDMA system model. In Chapter 5, we present the theoretical PAPR bounds by employing Golay complementary sequences for spreading and/or coding. Chapter 6 shows the simulation results to demonstrate our theoretical analysis. Finally, thesis conclusions are in Chapter 7.

Chapter 2

Background

2.1 M-PSK and M-QAM modulation schemes

M-PSK and M-QAM are memoryless digital modulation schemes. In these modulation schemes, the binary sequence is mapped into one of the $s_m(t)$, $1 \leq m \leq M$, signals regardless of the previously transmitted signals.

M-PSK uses M finite number of phases to represent the transmitted information. The M signal waveforms of M-PSK can be represented as [36]

$$\begin{aligned} s_m(t) &= Re[g(t)e^{j\frac{2\pi(m-1)}{M}}e^{j2\pi f_c t}], \quad m = 1, 2, ..., M \\ &= g(t)\cos[2\pi f_c t + \frac{2\pi}{M}(m-1)] \\ &= g(t)\cos(2\pi f_c t + \Theta_m) \end{aligned} \tag{2.1.1}$$

where

$$g(t) = \begin{cases} 1 & 0 \leq t \leq T_s \\ 0 & \text{otherwise} \end{cases}$$

T_s is the signaling interval. $\Theta_m = \frac{2\pi}{M}(m-1)$, $m = 1, 2, ...M$, is the M possible phases of the carrier that convey the transmitted information. If we denote the energy content of $s_m(t)$ by ξ_m,

$$\begin{aligned} \xi_m &= \int_0^{T_s} s_m^2(t)dt \\ &= \int_0^{T_s} g^2(t)\cos^2(2\pi f_c t + \Theta_m)dt. \end{aligned}$$

We can find that these M signal waveforms have equal energy. If we normalize ξ_m, $\xi_m = 1$. All of these M signals has equal unit energy.

The quadrature amplitude modulation (QAM) is an amplitude-phase keying modulation in which symbols are represented by different phases and amplitudes of a sinusoidal carrier. The corresponding M signal waveforms of M-QAM are expressed as [36]

$$\begin{aligned} s_m(t) &= Re[(A_{mi} + jA_{mq})g(t)e^{j2\pi f_c t}] \\ &= A_{mi}g(t)\cos 2\pi f_c t - A_{mq}g(t)\sin 2\pi f_c t, \quad m = 1, 2, ...M \end{aligned}$$

where A_{mi} and A_{mq} are the information-bearing signal amplitudes of the quadrature carriers and

$$g(t) = \begin{cases} 1 & 0 \leq t \leq T_s \\ 0 & \text{otherwise} \end{cases}.$$

Alternatively, the M-QAM signal waveforms can be expressed as

$$\begin{aligned} s_m(t) &= Re[r_m g(t) e^{j\Theta_m} e^{j2\pi f_c t}] \\ &= r_m g(t) \cos(2\pi f_c t + \Theta_m) \end{aligned}$$

where $r_m = \sqrt{A_{mi}^2 + A_{mq}^2}$ and $\Theta_m = \tan^{-1}(A_{mq}/A_{mi})$. From this expression, it is apparent that the M-QAM signal waveforms can be viewed as combined amplitude (r_m) and phase (Θ_m) modulation. Similarly, If we denote the energy content of $s_m(t)$ of M-QAM by ξ_m,

$$\begin{aligned} \xi_m &= \int_0^{T_s} s_m^2(t) dt \\ &= \int_0^{T_s} r_m^2 g^2(t) \cos^2(2\pi f_c t + \Theta_m) dt. \end{aligned}$$

A convenient way to represent M-PSK and M-QAM schemes is on a constellation diagram. This shows the points in the complex plane, where the real and imaginary axes are termed the in-phase (I) and quadrature (Q) axes respectively due to their 90 degrees separation. As shown above, if we normalize each signal's energy ξ_m

of M-PSK, each modulation symbol of M-PSK is positioned on a unique circle and transmitted with the same unit energy. Two common examples of M-PSK are binary phase-shift keying which uses two phases (BPSK or 2-PSK), and quadrature phase-shift keying (QPSK or 4-PSK) which uses four phases. Constellation diagrams of BPSK and QPSK are shown in Figure 2.1(a) and 2.1(b). A common example of M-QAM is 16-QAM. Its constellation diagram is shown in Figure 2.1(c) .

2.2 OFDM

Orthogonal frequency division multiplexing (OFDM) is a frequency division multiplexing (FDM) scheme that has been known since 1960's [19]. After that, the works of Chang and Gibby [26], Weinstein and Ebert [27], Peled and Ruiz [28], and Hirosaki [29] made OFDM both practical and attractive to various applications. So far, it has been standarized in many standards like Digital Audio Broadcasting (DAB) [30], Digital Video Broadcasting (DVB) [31], wireless local area networks (LAN) [32] and metropolitan area networks (MAN) [33], etc.

In Figure 2.2, the N message sequenes, $[a_0, a_1, ..., a_l, ..., a_{N-1}]$, form a frame, which is converted into a parallel form after serial to parallel (S/P) convertion, where a_l is modulating the lth subcarrier. The inverse fast Fourier transform (IFFT) module takes the parallel

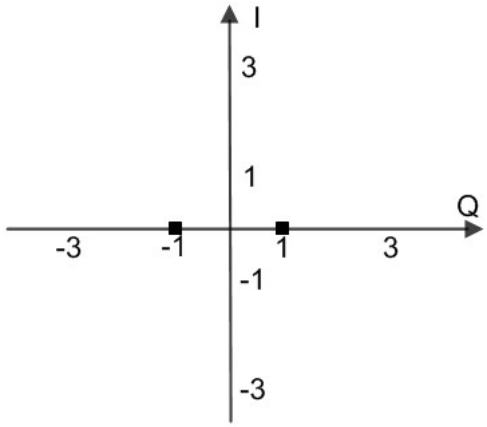

(a) BPSK

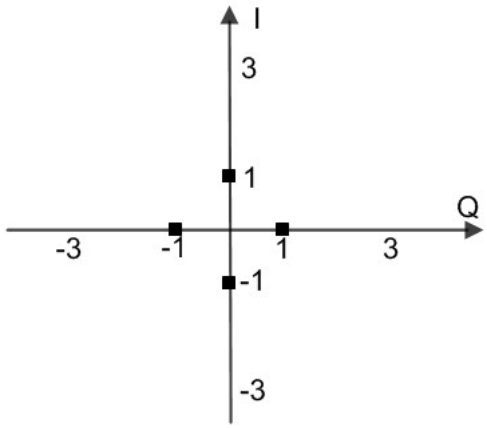

(b) QPSK

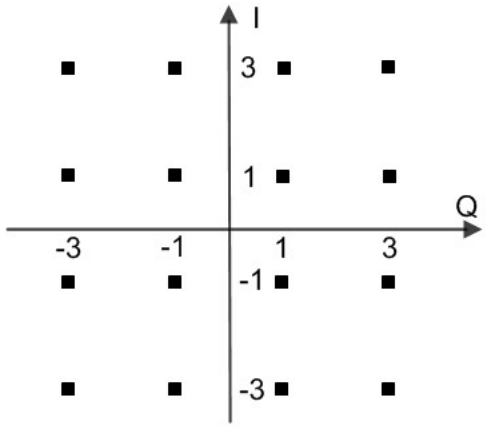

(c) 16-QAM

Figure 2.1: Examples of M-PSK and M-QAM modulation schemes

data and calculates N sampled time domain signals, $[s_0, s_1, ..., s_{N-1}]$, which are then converted by parallel to serial (P/S) and low-pass filtered to generate the continuous time domain signal $s(t)$. In a symbol duration, the baseband equivalent of the OFDM signal $s(t)$ in Figure 2.1 can be represented as

$$s(t) = \sum_{l=0}^{N-1} a_l e^{j2\pi(f_0 + \frac{l}{T_s})t} \tag{2.2.1}$$

where N is the number of subcarriers, f_0 is the lowest subcarrier frequency, T_s is the OFDM symbol duration, and a_l is the symbol modulating the subcarrier l.

The merits of OFDM as a transmission technique can be justified by comparative studies with single carrier systems. Compared with single carrier schemes, OFDM transmission uses a large number of orthogonal subcarriers to simultaneously transmit a large number of signals. Thus, although the subcarriers' spectra overlap in frequency domain, the individual signals on subcarriers can still be recovered. As a result, the system spectral efficiency is improved. Besides, OFDM can be viewed as using many slowly-modulated narrowband signals rather than one rapidly-modulated wideband signal. The low symbol rate makes the use of a guard interval between symbols affordable, making it possible to eliminate inter-symbol interference (ISI). What is more, these slowly-modulated narrowband signals have longer data symbol period. Thus, each subcarrier experiences

flat fading in multipath environments and is relatively simple to equalize. However, its main drawbacks are high sensitivity to frequency offset and high PAPR [34, 35, 36], which can put a high demand on the transmitter and receiver design of the OFDM system. Detailed overviews of OFDM and various high PAPR solutions can be found in [7].

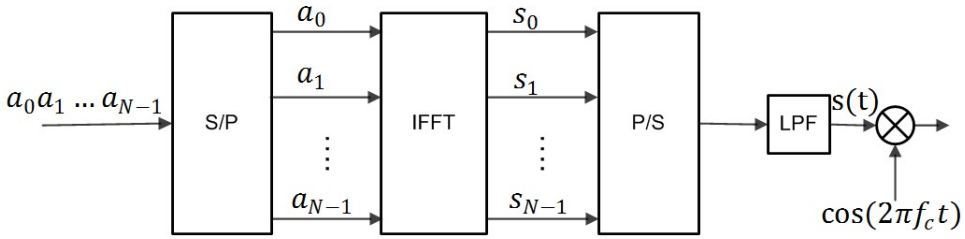

Figure 2.2: OFDM transmitter schematic

2.3 Spread spectrum technique

Spread spectrum technique was first developed for military communications in 1950's [37]. Compared with OFDM scheme mentioned above, spread spectrum is a means of transmission in which the signal occupies a bandwidth in excess of the minimum necessary to send the information. There are many benefits of spreading the spectrum. Some of them are anti-jamming, anti-interference, low probability of intercept, multiple user random access communications with selective addressing capability, high resolution ranging and accurate universal timing [38]. In this thesis, the focus will be on one of the spreading methods—direct-sequence spread spectrum (DSSS) only.

A detailed review of spread spectrum based communications can be found in [39, 40].

DSSS is the most widely used spread spectrum system so far. Its application areas includes global positioning system (GPS), European Galileo and Russian GLONASS satellite navigation systems, IEEE 802.11b [32] and IEEE 802.15.4 [41], etc. DSSS transmission is achieved by spreading the baseband data being transmitted with a specific spreading sequence. Since the data *absorbs* the increased rate due to spreading, a wider band signal is produced. But at the receiver side, this wider band signal can be exactly despreaded and recovered to the original data by using the same spreading sequence.

Based on this concept, if assigning different spreading sequences to different users, DSSS becomes a multiple access scheme called code division multiple access (CDMA). CDMA is capable of supporting multiple users to share a single channel, so it has a near-unity frequency reuse factor [42]. The direct and obvious advantages of this universal frequency reuse are the substantial increase in user capacity per unit bandwidth and the ability to use soft hand-off [42]. However, at the same time, the increased user capacity can lead CDMA suffering from inter-symbol interference (ISI) and multi-user interference (MUI). These interferences depend on the channel's characteristics and on the properties of the spreading sequences used. Thus, spreading sequences with good auto- and cross-correlation properties play an important role in improving the

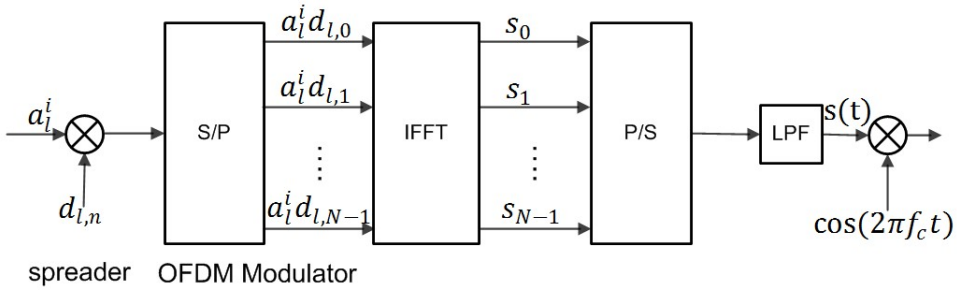

Figure 2.3: MC-CDMA transmitter scheme

performance of a CDMA system. The family of various spreading sequences are introduced in Chapter 9 of [43], while a range of related CDMA design aspects are covered in [44].

2.4 MC-CDMA

Multicarrier code division multiple access (MC-CDMA) has been proposed as a new multiple access scheme to satisfy the higher data rate transmissions over the wireless channels [1]. MC-CDMA combines OFDM and CDMA. It adopts the same transmitter structure as OFDM system. Also, it applies an orthogonal spreading matrix operation to user's information data, which is a form of direct-sequence CDMA (DS-CDMA). However, it applies the spreading in the frequency domain rather than in the time domain as in direct-sequence CDMA (DS-CDMA) [43].

2.4.1 MC-CDMA scheme

The MC-CDMA transmitter shown in Figure 2.3 is implemented by concatenating a DS-CDMA spreader and an OFDM transmitter. This figure shows the simplest case of an MC-CDMA transmitter in which only a single symbol is fully spread. For a general MC-CDMA transmitter, see Figure 4.1 in Chapter 4.

At the spreader, the ith information bit of the lth user a_l^i is spread in the frequency domain by the lth user's unique spreading sequence $[d_{l,0}, d_{l,1}, ..., d_{l,N-1}]$. The spread chips $[a_l^i d_{l,0}, a_l^i d_{l,1}, ..., a_l^i d_{l,N-1}]$ are then fed into the serial-to-parallel (S/P) block and IFFT is applied to these N parallel chips. The output values, $[s_0, s_1, ..., s_{N-1}]$, of the IFFT in Figure 2.3 are time domain samples in parallel form. After being parallel to serial (P/S) conversion, these time domain samples are low-pass-filtered and ready for transmission. Mathematically, the i-th data symbol of the l-th user's MC-CDMA transmission signal $s_l^i(t)$ can be written as [1, 45]

$$s_l^i(t) = \sum_{n=0}^{N-1} a_l^i d_{l,n} e^{j2\pi(f_0 + \frac{n}{T_s})t} \tag{2.4.1}$$

where

- N is the number of subcarriers
- a_l^i is the ith message symbol of the lth user
- $d_{l,n}$ represents the nth chip, $n = 0, ..., N-1$, of the spreading

sequence of the lth user

- f_0 is the lowest subcarrier frequency
- T_s is the symbol duration.

2.4.2 OFDM vs. MC-CDMA

As equation (2.2.1) indicated, in a signalling interval, OFDM modulation is a process to map N independent modulation symbols onto N different frequency subcarriers as shown in the power spectrum of OFDM system in Figure 2.4(a). However, by applying the spreading operation before OFDM modulator, MC-CDMA transmitter loads the same information data a_l^i over N subcarriers as shown in Figure 2.4(b). It helps to achieve a form of frequency diversity that makes MC-CDMA system robust against channel fading compared to OFDM system. Besides, the spreading sequence provides MC-CDMA system a multiple access capability [46]. Compared with OFDM based multiple access scheme known as orthogonal frequency division multiple access (OFDMA), MC-CDMA can provide relative fair and stable services to all users without elaborate multiuser scheduling [47, 48].

2.5 Peak-to-average power ratio (PAPR)

Peak-to-average power ratio (PAPR) is a measurement of a signal waveform. According to the definition of PAPR [49, 50, 51], the

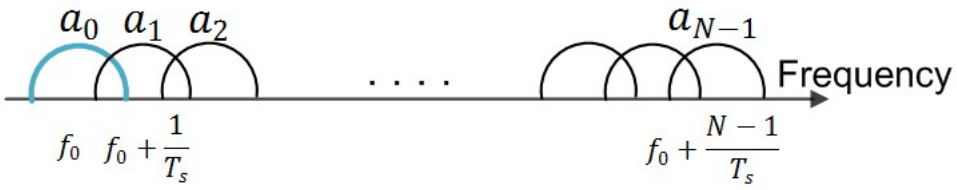

(a) Power spectrum of OFDM transmitted signal

(b) Power spectrum of MC-CDMA transmitted signal

Figure 2.4: Power spectrum of OFDM and MC-CDMA

PAPR of a signal $s(t)$ is defined as

$$\begin{aligned} \text{PAPR}(s(t)) &\triangleq \frac{\text{Peak Power}}{\text{Average Power}} = \frac{\max\limits_{0\le t\le T_s} |s(t)|^2}{\frac{1}{T_s}\int_0^{T_s} |s(t)|^2 dt}. \\ &= \frac{\max\limits_{0\le t\le T_s} |s(t)|^2}{E[|s(t)|^2]}. \end{aligned} \tag{2.5.1}$$

Example 1. Let $s(t)$ =sin(t), according to the definition in (2.5.1) above, we can get

$$\max_{0\le t\le 2\pi} |\sin(t)|^2 = 1$$

and

$$\begin{aligned}\frac{1}{2\pi}\int_0^{2\pi}|\sin(t)|^2\,dt &= \frac{1}{\pi}\int_0^{\pi}\sin^2(t)dt \\ &= \frac{1}{\pi}\int_0^{\pi}\frac{1}{2}(1-\cos(2t))dt \\ &= \frac{1}{2},\end{aligned}$$

then

$$\mathrm{PAPR}(\sin(t)) = 2.$$

In signal processing applications, PAPR is usually expressed in decibels. Consequently, the PAPR of the sine wave above is 3 dB.

As shown in equations (2.2.1) and (2.4.1), the multicarrier signals of both OFDM and MC-CDMA systems in time domain are the addition of N narrowband vector components. It is unavoidable that in some time instances, this sum is large and at other time is small, which means that the envelope of $s(t)$ is not stable and the peak value of the signal is substantially larger than the average value. Consequently, the high PAPR is caused [7].

There have been numerous efforts to reduce the envelope variations of $s(t)$ of both OFDM and MC-CDMA systems [23, 49] [52]-[56] [8]-[13]. Among these methods, coding is a specific approach of selecting good codewords to encode the information signal, so that the resultant signal can have the minimized or reduced PAPR for

transmission. For more studies of various coding schemes, see [43].

Chapter 3

Golay Complementary Sequences

3.1 Golay complementary sequences

Golay complementary sequences are one of the widely studied sequences used to cope with the high PAPR in multicarrier communication systems. It was found in 1961 as a set of complementary series [22] while Golay was working on the optical problem of spectometry.

Let $\mathbf{u} = (u_0, u_1, ..., u_{N-1})$ be a sequence of length $N = 2^m$, where m is a positive integer. Each element of $\mathbf{u}$ is in the integer ring $\mathbb{Z}_q = \{0, 1, ..., q-1\}$, where q is an even positive integer. The aperiodic autocorrelation of $\mathbf{u}$ is defined by

$$\rho_{\mathbf{u}}(\tau) = \sum_{i=0}^{N-1-\tau} \omega^{u_i - u_{i+\tau}}, \quad 0 \leq \tau \leq N-1 \tag{3.1.1}$$

where $\omega = e^{j\frac{2\pi}{q}}$. A q-ary sequence pair $(\mathbf{u}, \mathbf{v})$ of length N is called a *Golay complementary pair* if $\rho_{\mathbf{u}}(\tau) + \rho_{\mathbf{v}}(\tau) = 0$ for all $\tau \neq 0$, and $\mathbf{u}$ (or $\mathbf{v}$) is called a *Golay (complementary) sequence* [22].

For the sequence $\mathbf{u}$, we can define its *associated polynomial* $D_{\mathbf{u}}(z)$ as

$$D_{\mathbf{u}}(z) = \sum_{i=0}^{N-1} \omega^{u_i} z^i \tag{3.1.2}$$

where z lies on the unit circle in a complex plane, i.e., $z \in \{e^{j2\pi t} | 0 \leq t < 1,\ j = \sqrt{-1}\}$. Then, the Golay complementary pair ($\mathbf{u}$,$\mathbf{v}$) satisfies [57]

$$|D_{\mathbf{u}}(z)|^2 + |D_{\mathbf{v}}(z)|^2 = 2N. \tag{3.1.3}$$

In particular, for a Golay sequence $\mathbf{u}$, from the above equation, we have

$$|D_{\mathbf{u}}(z)|^2 \leq 2N. \tag{3.1.4}$$

Then the average energy of a Golay sequence $\mathbf{u}$ can be obtained as

$$E[|\mathbf{u}|^2] = \sum_{n=0}^{N-1} |u_n|^2 = \rho_{\mathbf{u}}(0) = N.$$

So, according to the definition of PAPR in equation (2.5.1), the PAPR of a Golay sequence $\mathbf{u}$ is 2 (3 dB).

Example 2. Let $q = 2$, then each element of a Golay sequence is in $\mathbb{Z}_2 = \{0, 1\}$. Assuming Golay sequences $\mathbf{u} = [\ 0 \quad 0 \quad 0 \quad 1 \quad 0 \quad 0 \quad 1 \quad 0]$, $\mathbf{v} = [\ 0 \quad 1 \quad 0 \quad 0 \quad 0 \quad 1 \quad 1 \quad 1\ ]$, the aperiodic autocorrelation of $\mathbf{u}$ can be obtained as

$$\rho_{\mathbf{u}} = \sum_{i=0}^{7-\tau} \omega^{u_i - u_{i+\tau}} = \ (8, \ -1, \ 0, \ 3, \ 0, \ 1, \ 0, \ 1) \ , \ \tau = 0, 1, ...7.$$

Correspondently, the aperiodic autocorrelation of $\mathbf{v}$ is $(8, 1, 0, -3, 0, -1, 0, -1)$. It is evident that their aperiodic autocorrelation sum is zero when $\tau \neq 0$, so $\{\mathbf{u}, \mathbf{v}\}$ is a Golay complementary pair (GCP).

Popović showed that the PAPR of any Golay complementary sequences is bounded by a value of two (or 3 dB) [56]. Davis and Jedwab [23] reported that Golay sequences can be used as a precoder for OFDM in order to bound the PAPR within a ratio of two (or 3 dB) as well as additionally to provide some error correction capability.

3.2 Direct construction of Golay complementary sequences

Let m be a positive integer, q be a even positive integer and π be a permutation in $\{0, 1, ..., m-1\}$. Standard q-ary Golay complementary sequences of length $N = 2^m$ can be constructed in the form of a Boolean function [23], i.e.

$$f(x_0, ..., x_{m-1}) = \frac{q}{2} \sum_{i=0}^{m-2} x_{\pi(i)} x_{\pi(i+1)} + \sum_{i=0}^{m-1} c_i x_i + e \qquad (3.2.1)$$

where $\pi(i)$ is the ith element of a given permutation π, c_i, $e \in \mathbb{Z}_q = \{0, 1, ..., q-1\}$ and the addition is computed modulo q. Then for a Golay complementary sequence $\mathbf{u} = (u_0, u_1, ..., u_{N-1})$, the relationship between $u_n \in \mathbf{u}$, $0 \leq n \leq N-1$, and f is

$$u_n = f(x_0, x_1, ..., x_{m-1}) \tag{3.2.2}$$

and $x_k \in [x_0, x_1, ..., x_{m-1}]$ can be obtained from

$$n = \sum_{k=0}^{m-1} x_k \cdot 2^k, \tag{3.2.3}$$

where n is the subscript of u_n. This construction method gives a set of $(m!/2)q^{m+1}$ distinct Goaly complementary sequences of length $N = 2^m$.

In (3.2.1), if we fix π and e, we can generate 2^m Golay complementary sequences for varying c_i, where each pair is mutually orthogonal.

Example 3. If we take $m = 3$, $q = 2$, $\pi = \{0, 1, 2\}$ and $e = 0$, we can get the Golay complementary sequences using the following steps.

Note: there are 6 types of permutations of $\{0, 1, 2\}$. They are: $\{0, 1, 2\}$, $\{0, 2, 1\}$, $\{1, 0, 2\}$, $\{1, 2, 0\}$, $\{2, 0, 1\}$, $\{2, 1, 0\}$. Among them, we choose $\pi = \{0, 1, 2\}$ in this example.

Step1, as we denote the first element of a Golay sequence $\mathbf{u}$ as u_0, $n = 0$.

Step 2, since $n = 0$, we can get the values of $[x_0, x_1, x_2]$ from the

equation (3.2.3) as following

$$\begin{aligned} n &= x_0 \cdot 2^0 + x_1 \cdot 2^1 + x_2 \cdot 2^2 \\ 0 &= 0 \cdot 2^0 + 0 \cdot 2^1 + 0 \cdot 2^2. \end{aligned}$$

Therefore, $x_0 = 0$, $x_1 = 0$, $x_2 = 0$.

Step 3, since $\pi = \{0, 1, 2\}$, then $\pi(0) = 0$, $\pi(1) = 1$ and $\pi(2) = 2$. Therefore, $x_{\pi(0)} = x_0$, $x_{\pi(1)} = x_1$ and $x_{\pi(2)} = x_2$. Hence,

$$\begin{aligned} f(x_0, x_1, x_2) &= \frac{q}{2} \sum_{i=0}^{m-2} x_{\pi(i)} x_{\pi(i+1)} + \sum_{i=0}^{m-1} c_i x_i + e \\ &= \frac{2}{2} (x_0 x_1 + x_1 x_2) + c_0 x_0 + c_1 x_1 + c_2 x_2 + 0. \end{aligned} \quad (3.2.4)$$

For c_0, c_1, $c_2 \in \mathbb{Z}_2 = \{0, 1\}$, we can get 8 possible combinations of $[c_0, c_1, c_2]$. They are

$$\begin{matrix} 0 & 0 & 0 \\ 0 & 0 & 1 \\ 0 & 1 & 0 \\ 0 & 1 & 1 \\ 1 & 0 & 0 \\ 1 & 0 & 1 \\ 1 & 1 & 0 \\ 1 & 1 & 1 \end{matrix} .$$

If we bring the values of $[x_0, x_1, x_2]$ and each combination of $[c_0, c_1, c_2]$ back to (3.2.4), we can get 8 possible values of the first element u_0 of a Golay complementary sequence $\mathbf{u}$,

$$\mathbf{u}_0 = \begin{bmatrix} 0 & 0 & 0 & 0 & 0 & 0 & 0 & 0 \end{bmatrix}^T .$$

Similarly, we can also get $\mathbf{u}_1$, $\mathbf{u}_2$, ..., $\mathbf{u}_7$. Then, 8 Golay complementary sequences of length 8 are

$\mathbf{u}_0$	$\mathbf{u}_1$	$\mathbf{u}_2$	$\mathbf{u}_3$	$\mathbf{u}_4$	$\mathbf{u}_5$	$\mathbf{u}_6$	$\mathbf{u}_7$
0	0	0	1	0	0	1	0
0	1	0	0	0	1	1	1
0	0	1	0	0	0	0	1
0	1	1	1	0	1	0	0
0	0	0	1	1	1	0	1
0	1	0	0	1	0	0	0
0	0	1	0	1	1	1	0
0	1	1	1	1	0	1	1

,

where each row is a Golay complementary sequence $\mathbf{u}= [u_0, u_1, ..., u_7]$. After BPSK modulation, a set of BPSK modulated orthogonal Golay complementary sequences of length 8 can be obtained as

$$H = \begin{matrix} + & + & + & - & + & + & - & + \\ + & - & + & + & + & - & - & - \\ + & + & - & + & + & + & + & - \\ + & - & - & - & + & - & + & + \\ + & + & + & - & - & - & + & - \\ + & - & + & + & - & + & + & + \\ + & + & - & + & - & - & - & + \\ + & - & - & - & - & + & - & - \end{matrix}.$$

It is easy to check that

$$H \cdot H^T = 8I$$

where I is a 8×8 identity matrix. Hence, each pair of the Golay sequences in the set H is orthogonal. In general, we can obtain an orthogonal set of Golay sequences of length 2^m for a spreading matrix.

Using quaternary Golay sequences, Rößing and Tarokh [24, 25] gave the construction of 16-QAM Golay sequences $q(\mathbf{u}, \mathbf{v}) = (q_0, q_1, ...q_{N-1})$ that can be summarized as follows [25]

$$q_i = \alpha e^{j\pi/4} \varepsilon^{u_i} + \beta e^{j\pi/4} \varepsilon^{v_i} \tag{3.2.5}$$

where $\alpha, \ \beta \ \in \mathbb{R}$, $\varepsilon = e^{j2\pi/4}$ and $\mathbf{u} = (u_0, u_1, ..., u_{N-1})$, $\mathbf{v} = (v_0, v_1, ..., v_{N-1})$ are quaternary Golay sequences. If all the 16-QAM symbols are equiprobable, then $\alpha = 2/\sqrt{5}$, $\beta = 1/\sqrt{5}$ for the constellation having the unit average energy [24].

Let $\mathbf{w}$ denote the 16-QAM Golay sequence $\mathbf{w} = q(\mathbf{u}, \mathbf{v})$, we can define two different sets of $\mathbf{w}$'s, e.g., $\mathcal{A}$ and $\mathcal{B}$,

- In set $\mathcal{A}$ ($\mathbf{w} \in \mathcal{A}$), $\mathbf{u}$ and $\mathbf{v}$ are Golay sequences, but not necessarily a complementary pair. Then PAPR($\mathbf{w}$) ≤ 3.6 [24].
- In set $\mathcal{B}$ ($\mathbf{w} \in \mathcal{B}$), $\mathbf{u}$ and $\mathbf{v}$ form a Golay complementary pair. Then PAPR($\mathbf{w}$) ≤ 2 [24].

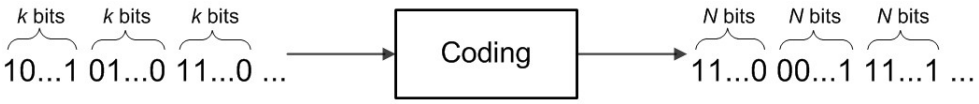

Figure 3.1: Block coding diagram

Therefore, in the set $\mathcal{A}$, we have $((m!/2)4^{m+1})^2$ [24] 16-QAM Golay complementary sequences having the PAPR bounded by 3.6. In the set $\mathcal{B}$, $(m!)4^{m+2}$ [24] 16-QAM Golay sequences have the PAPR bounded by 2.0.

3.3 Code rate of Golay complementary sequences

In block coding diagram as shown in Figure 3.1, one of the 2^k messages, each representing a binary sequence of length k, called the *information sequence*, is mapped to a binary sequence of length N, called the *codeword*. Code rate represents the proportion of the data-stream that is useful. It is denoted by R and is given by

$$R = \frac{k}{N}.$$

If there are S codewords, these S codewords can be used to encode 2^k binary messages of length k. Consequently, $2^k = S$. Then

$$k \;=\; \lfloor \log_2 S \rfloor .$$

In this thesis, QPSK, 16-QAM ($\mathcal{A}$) and 16-QAM ($\mathcal{B}$) Golay com-

plementary sequences are used for the coding scheme, which is employed for reducing the PAPR of MC-CDMA in Chapter 5. For a given m, since we can generate $S = (m!/2)4^{m+1}$ QPSK modulated quaternary Golay complementary sequences of length $N = 2^m$, the code rate of QPSK modulated quaternary Golay sequences can be obtained as

$$\begin{aligned} R &= \frac{k}{N} \\ &= \frac{\lfloor \log_2 S \rfloor}{2^m} \\ &= \frac{\lfloor \log_2 (m!/2) \rfloor + 2m + 2}{2^m}. \end{aligned}$$

Likewise, for a given m, the code rate of 16-QAM ($\mathcal{A}$) Golay sequences is

$$R = \frac{\lfloor \log_2 [(m!/2)4^{m+1}]^2 \rfloor}{2^m}$$

and the code rate of 16-QAM ($\mathcal{B}$) Golay sequences is

$$R = \frac{\lfloor \log_2 (m!) 4^{m+2} \rfloor}{2^m}.$$

The code rates of QPSK, 16-QAM ($\mathcal{A}$) and 16-QAM ($\mathcal{B}$) Golay complementary sequences are caculated and shown in Table 3.1. When $m = 4$, we can find that code rates of these three types of Golay sequences are all below 1/2. It is unacceptable in most

Table 3.1: Code rates for coded MC-CDMA

m	1	2	3	4
QPSK	0.7500	0.7500	0.5991	0.4245
16-QAM ($\mathcal{A}$)	0.7500	0.7500	0.5366	0.4245
16-QAM ($\mathcal{B}$)	0.7500	0.5625	0.3933	0.2591

applications and hence it is better to use amplifier-back-off or other error correction codes [58].

Chapter 4

System Architecture

Table 4.1: Summary of notations

L	total number of users
K	number of spreading process, the codeword length of coded case
$\mathbf{a}^{(k)}$	L dimensional modulation symbol vector input to the kth spreading process
$\mathbf{a}_l$	the lth user's information vector/coded symbol of length K
$\mathbf{b}^k$	$1 \times N$ vector after kth spreading
C	$L \times N$ spreading matrix, each row is a binary Golay sequence of length N
N	the length of a Golay spreading sequence, spreading factor

4.1 Downlink MC-CDMA transmitter model

We consider an MC-CDMA system model shown in Figure 4.1. In Figure 4.1, L users actively transmit K modulation symbols in an OFDM symbol. Equivalently, the MC-CDMA system has K identical spreading processes, each of which spreads L modulation symbols. $\mathbf{a}^{(k)} = (a_0^{(k)}, a_1^{(k)}, ..., a_{L-1}^{(k)})$ is an L-dimensional modulation symbol vector input to the kth spreading process, where $a_l^{(k)}$

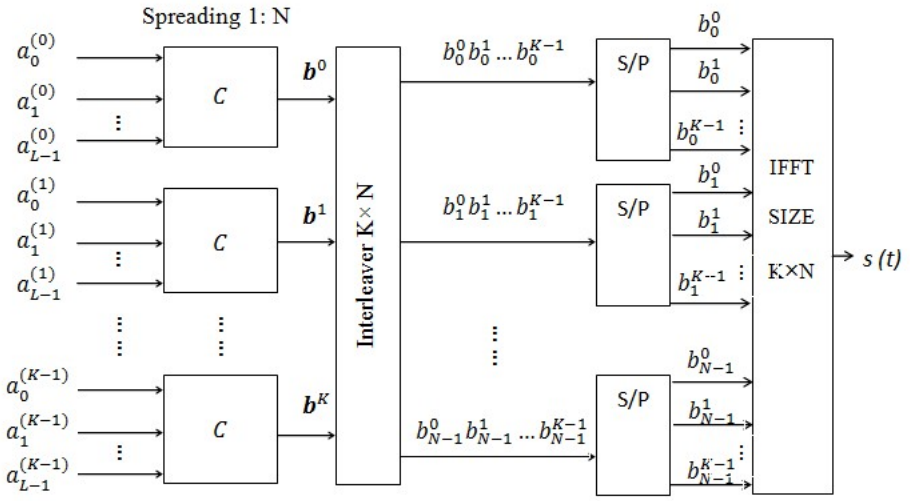

Figure 4.1: MC-CDMA system model

denotes the lth modulation symbol in the kth spreading process. $\mathbf{a}_l = (a_l^{(0)}, a_l^{(1)}, ..., a_l^{(K-1)})$ denotes the lth user's information vector of length K. C is an $L \times N$ $(L \leq N)$ spreading matrix. Each row l $(0 \leq l \leq L-1)$ of C contains the spreading sequence of user l, which is unique to the lth user. When each user$l$'s kth modulation symbol $a_l^{(k)}$ multiples its spreading sequence $\mathbf{d}_l = (d_{l,0}, d_{l,1}, ..., d_{l,N-1})$, $0 \leq l \leq L-1$, $a_l^{(k)}$ is spread N times in the frequency domain. The notations in the following chapters are summarized in Table 4.1. In order to achieve frequency diversity, we use the $K \times N$ interleaver after the spreading processes. As Figure 4.1 shown, the $K \times N$ interleaver stores the output $\mathbf{b}^k(b_0^k b_1^k ... b_{N-1}^k)$,

$$\begin{aligned} b_0^k &= a_0^{(k)} d_{0,0} + a_1^{(k)} d_{1,0} + \cdots + a_{L-1}^{(k)} d_{L-1,0}, \\ b_1^k &= a_0^{(k)} d_{0,1} + a_1^{(k)} d_{1,1} + \cdots + a_{L-1}^{(k)} d_{L-1,1}, \\ &\vdots \\ b_{N-1}^k &= a_0^{(k)} d_{0,N-1} + a_1^{(k)} d_{1,N-1} + \cdots + a_{L-1}^{(k)} d_{L-1,N-1}, \end{aligned}$$

into a $K \times N$ matrix

$$\begin{matrix} b_0^0 & b_1^0 & ... & b_{N-1}^0 \\ b_0^1 & b_1^1 & ... & b_{N-1}^1 \\ . & . & ... & . \\ . & . & ... & . \\ . & . & ... & . \\ b_0^{K-1} & b_1^{K-1} & ... & b_{N-1}^{K-1} \end{matrix} .$$

Then output these data in N columns, they are $[b_0^0 b_0^1 ... b_0^K]$, $[b_1^0 b_1^1 ... b_1^K]$, ..., $[b_{N-1}^0 b_{N-1}^1 ... b_{N-1}^K]$. After serial to parallel conversion and inverse fast Fourier transform (IFFT), the MC-CDMA signal $s(t)$ is represented by

$$s(t) = \sum_{k=0}^{K-1} \sum_{n=0}^{N-1} \sum_{l=0}^{L-1} a_l^{(k)} \cdot d_{l,n} \cdot e^{j2\pi(Kn+k)t/T_s}, \quad 0 \le t \le T_s, \qquad (4.1.1)$$

where T_s is an OFDM symbol duration.

4.2 PAPR of MC-CDMA

For $s(t)$ in (4.1.1), by substituting $e^{j2\pi t/T_s}$ with z, we can get the associated polynomial $S(z)$ shown below

$$S(z) = \sum_{k=0}^{K-1} \sum_{n=0}^{N-1} \sum_{l=0}^{L-1} a_l^{(k)} \cdot d_{l,n} \cdot z^{(Kn+k)} \tag{4.2.1}$$

where $|z| = 1$. A simple approach made in [15] enables us to caculate the average power of the downlink MC-CDMA signal $S(z)$ as below

$$E[|S(z)|^2] = \sum_{k=0}^{K-1} \sum_{n=0}^{N-1} \sum_{l=0}^{L-1} \left| a_l^{(k)} \right|^2 |d_{l,n}|^2 .$$

Normalizing each user's modulation symbol, i.e., $\left| a_l^{(k)} \right|^2 = 1$ and $|d_{l,n}| = 1$, then the above equation becomes

$$E[|S(z)|^2] = K \cdot N \cdot L. \tag{4.2.2}$$

Consequently, from (2.5.1) and (4.2.2), the PAPR of $s(t)$ can be written as

$$\text{PAPR}(s(t)) = \frac{\max\limits_{|z|=1} |S(z)|^2}{K \cdot N \cdot L}. \tag{4.2.3}$$

In Chapter 5, based on the above downlink MC-CDMA transmitter's mathematical model and the Golay complementary sequences generated in Chapter 3, the theoretical analysis of the system's PAPR properties will be presented by employing Golay complementary sequences for spreading and/or coding.

Chapter 5

Theoretical Analysis

In this section, we develop the theoretical PAPR bounds for both uncoded and coded cases. Each row of the spreading matrix C in Figure 4.1 is a BPSK modulated binary Golay complementary sequence of length $N = 2^m$, i.e., each entry of C is ± 1, where $\pi = \{0, 1, ..., m-1\}$ and $q = 2$, $e = 0$ in (3.2.1). Moreover, we arrange the spreading matrix C in which a pair of row vectors $d_{2l'}$ and $d_{2l'+1}$ is a Golay complementary pair, where $0 \leq l' \leq \lfloor \frac{L}{2} \rfloor - 1$.

5.1 PAPR bounds using Golay complementary sequences for spreading

Theorem 1. Assuming each user transmits K modulation symbols, the PAPR bound of the MC-CDMA signal is

$$\mathrm{PAPR}(s_{M-\mathrm{PSK}}(t)) \leq \begin{cases} L \cdot K, & \text{if } L \text{ is even} \\ \frac{K}{L} \cdot (L - 1 + \sqrt{2})^2, & \text{if } L \text{ is odd,} \end{cases} \tag{5.1.1}$$

$$\mathrm{PAPR}(s_{M-\mathrm{QAM}}(t)) \leq \begin{cases} \frac{3(\sqrt{M}-1)}{\sqrt{M}+1} \cdot L \cdot K, & \text{if } L \text{ is even} \\ \frac{3(\sqrt{M}-1)}{\sqrt{M}+1} \cdot \frac{K}{L} \cdot (L - 1 + \sqrt{2})^2, & \text{if } L \text{ is odd.} \end{cases} \tag{5.1.2}$$

Proof. At the beginning, we assume that each user transmits a single modulation symbol in an OFDM symbol, that is, $K = 1$. Let $a_l^{(0)}$ be the lth user's modulation symbol, and $d_{l,n}$ be the nth element of the lth spreading sequence, where $0 \leq l \leq L-1$, $0 \leq n \leq N-1$. Note that the lth spreading sequence $\mathbf{d}_l = (d_{l,0}, ..., d_{l,N-1})$ is a Golay complementary sequence of length N, where $d_{l,n} \in \{-1, +1\}$. Then, from (4.2.1), the associate polynomial of MC-CDMA signal can be written as

$$S_0(z) = \sum_{n=0}^{N-1} \sum_{l=0}^{L-1} a_l^{(0)} d_{l,n} z^n = \sum_{l=0}^{L-1} a_l^{(0)} D_l(z) \tag{5.1.3}$$

where $D_l(z) = \sum_{n=0}^{N-1} d_{l,n} z^n$ is the associated polynomial of $\mathbf{d}_l$ as defined in (3.1.2). Then,

$$
\begin{aligned}
|S_0(z)|^2 &= \sum_{l=0}^{L-1}\sum_{h=0}^{L-1} a_l^{(0)} a_h^{*(0)} D_l(z) D_h^*(z) \\
&\leq \sum_{l=0}^{L-1}\sum_{h=0}^{L-1} \left| a_l^{(0)} a_h^{*(0)} D_l(z) D_h^*(z) \right| \\
&\leq \max_{0\leq l\leq L-1} \left| a_l^{(0)} \right|^2 \cdot \sum_{l=0}^{L-1}\sum_{h=0}^{L-1} |D_l(z)| \cdot |D_h^*(z)| \\
&\leq \max_{0\leq l\leq L-1} \left| a_l^{(0)} \right|^2 \cdot \sum_{l=0}^{L-1} |D_l(z)| \cdot \sum_{h=0}^{L-1} |D_h^*(z)| \\
&= \max_{0\leq l\leq L-1} \left| a_l^{(0)} \right|^2 \cdot \left(\sum_{l=0}^{L-1} |D_l(z)| \right)^2 . \qquad (5.1.4)
\end{aligned}
$$

Since $\mathbf{d}_{2l'}$ and $\mathbf{d}_{2l'+1}$, $0 \leq l' \leq \left\lfloor \frac{L}{2} \right\rfloor - 1$, form a Golay complementary pair,

$$|D_{2l'}(z)|^2 + |D_{2l'+1}(z)|^2 = 2N.$$

Also, $|D_{2l'}(z)| \cdot |D_{2l'+1}(z)| \leq \frac{|D_{2l'}(z)|^2 + |D_{2l'+1}(z)|^2}{2} = N$. Therefore, it is straightforward that

$$
\begin{aligned}
|D_{2l'}(z)| + |D_{2l'+1}(z)| &= \sqrt{\left(|D_{2l'}(z)| + \left| D_{2l'+1}(z) \right| \right)^2} \\
&= \sqrt{|D_{2l'}(z)|^2 + \left| D_{2l'+1}(z) \right|^2 + 2\,|D_{2l'}(z)| \left| D_{2l'+1}(z) \right|} \\
&\leq \sqrt{2N + 2N} \\
&= 2\sqrt{N}
\end{aligned}
$$

If L is even, $\frac{L}{2}$ pairs of the spreading sequences form the Golay complementary pairs. Then,

$$\begin{aligned}\sum_{l=0}^{L-1}|D_l(z)| &= \sum_{l'=0}^{\lfloor\frac{L}{2}\rfloor-1}\left(|D_{2l'}(z)|+|D_{2l'+1}(z)|\right)\\ &\leq 2\sqrt{N}\cdot\frac{L}{2}=\sqrt{N}\cdot L \qquad (5.1.5)\end{aligned}$$

On the other hand, if L is odd, $\frac{L-1}{2}$ pairs are Golay complementary pairs. Then,

$$\begin{aligned}\sum_{l=0}^{L-1}|D_l(z)| &= \sum_{l'=0}^{\lfloor\frac{L}{2}\rfloor-1}\left(|D_{2l'}(z)|+|D_{2l'+1}(z)|\right)+|D_{L-1}(z)|\\ &\leq 2\sqrt{N}\cdot\frac{L-1}{2}+|D_{L-1}(z)|\,.\end{aligned}$$

According to (3.1.4),

$$|D_{L-1}(z)|\leq\sqrt{2N}.$$

Consequently, we can get

$$\begin{aligned}\sum_{l=0}^{L-1}|D_l(z)| &\leq 2\sqrt{N}\cdot\frac{L-1}{2}+\sqrt{2N}\\ &= \sqrt{N}\cdot(L-1)+\sqrt{2N}. \qquad (5.1.6)\end{aligned}$$

From (5.1.4), (5.1.5), and (5.1.6), we get

$$|S_0(z)|^2 \leq \begin{cases} \max\limits_{0\leq l\leq L-1} \left|a_l^{(0)}\right|^2 \cdot NL^2, & \text{if } L \text{ is even} \\ \max\limits_{0\leq l\leq L-1} \left|a_l^{(0)}\right|^2 \cdot N \cdot (L-1+\sqrt{2})^2, & \text{if } L \text{ is odd.} \end{cases} \tag{5.1.7}$$

Let a_l be either an M-PSK or an M-QAM modulation symbol. Then it is known that $\max\limits_l \left|a_l^{(0)}\right|^2 = 1$ for M-PSK. For M-QAM, by normalizing the average energy of each symbol, we can get $\max\limits_l \left|a_l^{(0)}\right|^2 = \frac{3(\sqrt{M}-1)}{\sqrt{M}+1}$ [36]. Thus, from (5.1.7) and (4.2.3), we can easily get the PAPR bounds of this system when $K = 1$.

$$\begin{aligned} \text{PAPR}(s_{M-\text{PSK}}(t)) &\leq \begin{cases} L, & \text{if } L \text{ is even} \\ \frac{1}{L} \cdot (L-1+\sqrt{2})^2, & \text{if } L \text{ is odd,} \end{cases} \\ \text{PAPR}(s_{M-\text{QAM}}(t)) &\leq \begin{cases} \frac{3(\sqrt{M}-1)}{\sqrt{M}+1} \cdot L, & \text{if } L \text{ is even} \\ \frac{3(\sqrt{M}-1)}{\sqrt{M}+1} \cdot \frac{1}{L} \cdot (L-1+\sqrt{2})^2, & \text{if } L \text{ is odd.} \end{cases} \end{aligned}$$

Generally, if we define

$$A_k(z) = \sum_{n=0}^{N-1} \sum_{l=0}^{L-1} a_l^{(k)} \cdot d_{l,n} z^n, \tag{5.1.8}$$

then $S(z)$ in (4.2.1) can be written as

$$S(z) = \sum_{k=0}^{K-1} A_k(z^K) \cdot z^k. \tag{5.1.9}$$

Let P_0 be the right-hand side of (5.1.7), i.e. $|S_0(z)|^2 \leq P_0$. Comparing (5.1.8) with (5.1.3), we can find that$|A_0(z)|^2 = |S_0(z)|^2 \leq P_0$. Since $a_l^{(k)}$ of each spreading process k is the same of either an M-PSK or an M-QAM modulation symbol in (5.1.8), we can get from (5.1.3) and (5.1.7) that

$$A_k(z) \leq P_0$$

for every k. By the Cauchy-Schwarz inequality,

$$\begin{aligned} |S(z)|^2 &= \left| \sum_{k=0}^{K-1} A_k(z^K) z^k \right|^2 \\ &\leq \sum_{k=0}^{K-1} |A_k(z^K)|^2 \cdot \sum_{k=0}^{K-1} |z^k|^2 \\ &\leq K \cdot \sum_{k=0}^{K-1} P_0 \\ &= K^2 \cdot P_0 \end{aligned}$$

where $|z| = 1$. Accordingly, together with (4.1.5) and (4.1.6), we can simply get the overall PAPR bounds given in Theorem 1.

□

Remark 1 : From Theorem 1, we found that the PAPR bounds depend on the number of active users L and the number of the modulation symbols K of each user in an OFDM symbol, regardless of spreading factor N.

5.2 PAPR bounds using Golay complementary sequences for spreading and coding

In this section, we study the PAPR bounds of coded MC-CDMA systems where Golay complementary sequences are used for both spreading and coding. In the following, we adopt both QPSK and 16-QAM Golay complementary sequences of length $K = 2^m$ as the codewords to encode each transmitted data.

Theorem 2. Assume a coding scheme by QPSK Golay complementary sequences. That is, the lth user's data $\mathbf{a}_l = (a_l^{(0)}, a_l^{(1)}, ..., a_l^{(K-1)})$ is a QPSK complementary sequence of length K. Then, the PAPR bound of the system is

$$\text{PAPR}(s(t)) \leq \begin{cases} 2L, & \text{if } L \text{ is even} \\ \frac{2}{L} \cdot (L - 1 + \sqrt{2})^2, & \text{if } L \text{ is odd.} \end{cases} \tag{5.2.1}$$

Proof. Note that $A_k(z) = \sum_{l=0}^{L-1} a_l^{(k)} D_l(z)$, where $D_l(z) = \sum_{n=0}^{N-1} d_{l,n} z^n$, $0 \leq k \leq K-1$. Then, from (5.1.9),

$$\begin{aligned} S(z) &= \sum_{k=0}^{K-1} \left(\sum_{l=0}^{L-1} a_l^{(k)} D_l(z^K) \right) \cdot z^k \\ &= \sum_{l=0}^{L-1} D_l(z^K) \cdot G_l(z) \end{aligned}$$

where $G_l(z) = \sum_{k=0}^{K-1} a_l^{(k)} z^k$. Then,

$$\begin{aligned} |S(z)| &= \sum_{l=0}^{L-1} |D_l(z^K) \cdot G_l(z)| \\ &\leq \sum_{l=0}^{L-1} |D_l(z^K)| \cdot |G_l(z)| \\ &\leq \max_{0 \leq l \leq L-1} |G_l(z)| \cdot \sum_{l=0}^{L-1} |D_l(z^K)| \end{aligned}$$

where

$$\sum_{l=0}^{L-1} |D_l(z^K)| \leq \begin{cases} \sqrt{N} \cdot L, & \text{if } L \text{ is even} \\ \sqrt{N} \cdot (L-1) + \sqrt{2N}, & \text{if } L \text{ is odd} \end{cases}$$

and $G_l(z)$ here is a form of the associated polynomial of the lth user's coded symbol. Since $\mathbf{a}_l$ is assumed to be a QPSK Golay complementary sequence of length K, we can find $|G_l(z)| \leq \sqrt{2K}$ from (3.1.4). Thus,

$$|S(z)| \leq \begin{cases} \sqrt{2K} \cdot \sqrt{N} \cdot L & \text{if } L \text{ is even} \\ \sqrt{2K} \cdot \sqrt{N} \cdot (L - 1 + \sqrt{2}) & \text{if } L \text{ is odd.} \end{cases}$$

Therefore,

$$|S(z)|^2 \leq \begin{cases} 2K \cdot N \cdot L^2 & \text{if } L \text{ is even} \\ 2K \cdot N \cdot (L - 1 + \sqrt{2})^2 & \text{if } L \text{ is odd.} \end{cases}$$

Then from $\mathrm{PAPR}(s(t)) = \frac{\max_{|z|=1}|S(z)|^2}{K \cdot N \cdot L}$ in (4.2.3), we can obtain the QPSK Golay complementary sequences coded PAPR bound of (5.2.1).

□

Likewise, we can derive the PAPR bounds when encoding each transmitted data as 16-QAM Golay complementary sequences.

Theorem 3.Assume a coding scheme by 16-QAM Golay Complementary sequence. That is, the lth user's data $\mathbf{a}_l = (a_l^{(0)}, a_l^{(1)}, ..., a_l^{(K-1)})$ is a 16-QAM complementary sequence of length K. If $\mathbf{a}_l \in \mathcal{A}$, then the PAPR bound of MC-CDMA signal is

$$\mathrm{PAPR}(s(t)) \leq \begin{cases} 3.6L, & \text{if } L \text{ is even} \\ \frac{3.6}{L} \cdot (L - 1 + \sqrt{2})^2, & \text{if } L \text{ is odd} \end{cases}, \qquad (5.2.2)$$

If $\mathbf{a}_l \in \mathcal{B}$, then,

$$\mathrm{PAPR}(s(t)) \leq \begin{cases} 2L, & \text{if } L \text{ is even} \\ \frac{2}{L} \cdot (L - 1 + \sqrt{2})^2, & \text{if } L \text{ is odd} \end{cases}. \qquad (5.2.3)$$

Proof. From above, we know that

$$|S(z)| \leq \max_{0\leq l\leq L-1} |G_l(z)| \cdot \sum_{l=0}^{L-1} |D_l(z^K)|$$

where

$$\sum_{l=0}^{L-1} |D_l(z^K)| \leq \begin{cases} \sqrt{N}\cdot L, & \text{if } L \text{ is even} \\ \sqrt{N}\cdot (L-1)+\sqrt{2N}, & \text{if } L \text{ is odd} \end{cases}$$

and $G_l(z)$ is a form of the associated polynomial of the lth user's coded symbol. As shown in Chapter 3, if we let $\mathbf{a}_l$ be a 16-QAM Golay ($\mathcal{A}$) sequence of length K, then $|G_l(z)| \leq \sqrt{3.6K}$; if we let $\mathbf{a}_l$ be a 16-QAM Golay ($\mathcal{B}$) complementary sequence of length K, then $|G_l(z)| \leq \sqrt{2K}$. Consequently,

if $\mathbf{a}_l \in \mathcal{A}$,

$$|S(z)|^2 \leq \begin{cases} 3.6K\cdot N\cdot L^2 & \text{if } L \text{ is even} \\ 3.6K\cdot N\cdot (L-1+\sqrt{2})^2 & \text{if } L \text{ is odd.} \end{cases}$$

if $\mathbf{a}_l \in \mathcal{B}$,

$$|S(z)|^2 \leq \begin{cases} 2K\cdot N\cdot L^2 & \text{if } L \text{ is even} \\ 2K\cdot N\cdot (L-1+\sqrt{2})^2 & \text{if } L \text{ is odd.} \end{cases}$$

Then from (4.2.3), we can get the PAPR bounds of (5.2.2) and (5.2.3).

□

Remark 2 : Theorems 2 and 3 reveal that if $\mathbf{a}_l$, $0 \leq l \leq K-1$, is a codeword from QPSK or 16-QAM Golay complementary sequences of length K, the PAPR bound does not increase along with K anymore. The bound depends on the number of active users L only. In particular, if we compare Theorems 1, 2 and 3, when $\mathbf{a}_l$ is a QPSK Golay sequence or a 16-QAM Golay sequence in set $\mathcal{B}$, then the theoretical PAPR bounds of coded MC-CDMA in (5.2.1) and (5.2.3) are identical to that of uncoded MC-CDMA when $K = 2$ in (5.1.1). For large K, we can therefore achieve the PAPR reduction by employing the coding schemes.

Chapter 6

Simulation Results

In this section, we show our simulation results to demonstrate the theoretical PAPR properties of uncoded and coded MC-CDMA systems. Various values of spreading processes K and spreading sequence lengths $N = 2^m$ for our simulation are summarized in Table 6.1.

In our simulation, we have tested 10^5 OFDM symbols to measure the 99.9% PAPR or PAPR_0, where $\Pr[\text{PAPR} > \text{PAPR}_0] = 10^{-3}$, for both uncoded and coded MC-CDMA systems. For uncoded cases, we generated each active user's uncoded QPSK or 16-QAM modulation symbols randomly. For coded cases, we randomly selected

Table 6.1: Simulation parameters

	uncoded	coded
K	1,2	4,8,16
N	8,16,32	8,16,32
Subcarriers($K \times N$)	8,16,32,64	32,64,128,256,512

each codeword from the whole set of QPSK and 16-QAM Golay complementary sequences. Considering the code rates as shown in Table 3.1, we constrain the maximum length of the codewords to 16 so that the system can maximally support 512 subcarriers.

Figures 6.1, 6.2, 6.3 and 6.4 show the uncoded QPSK and 16-QAM 99.9% PAPRs for $K = 1$ and 2, respectively, with respect to the successively increased active user number L, along with the uncoded theoretical PAPR bounds for comparison. When K increases, it is shown that both theoretical PAPR bounds and 99.9% PAPRs increase accordingly. In addition, these figures show that the 99.9% PAPRs and theoretical PAPR bounds do not increase when N increases. They just depend on the number of active users L only.

Figures 6.5, 6.6 and 6.7 show the coding case that each active user's transmitted symbols are encoded as QPSK Golay sequences, 16-QAM Golay sequences ($\mathcal{A}$) and ($\mathcal{B}$) of length $K = 16$, respectively. The simulation results confirm that both PAPR bounds and 99.9% PAPRs of coded cases indepent of the spreading factor N.

In order to clearly demonstrate the coded PAPR bounds and 99.9% PAPRs have no dependency on the spreading factor K, in the following, we start to compare the 99.9% PAPRs of the uncoded cases when $K = 2$ together with the 99.9% PAPRs of coded cases with various values of K. Figure 6.8 displays 99.9% PAPR of uncoded and coded MC-CDMA with $N = 16$. In uncoded MC-CDMA, each user transmits two QPSK modulated symbols in an

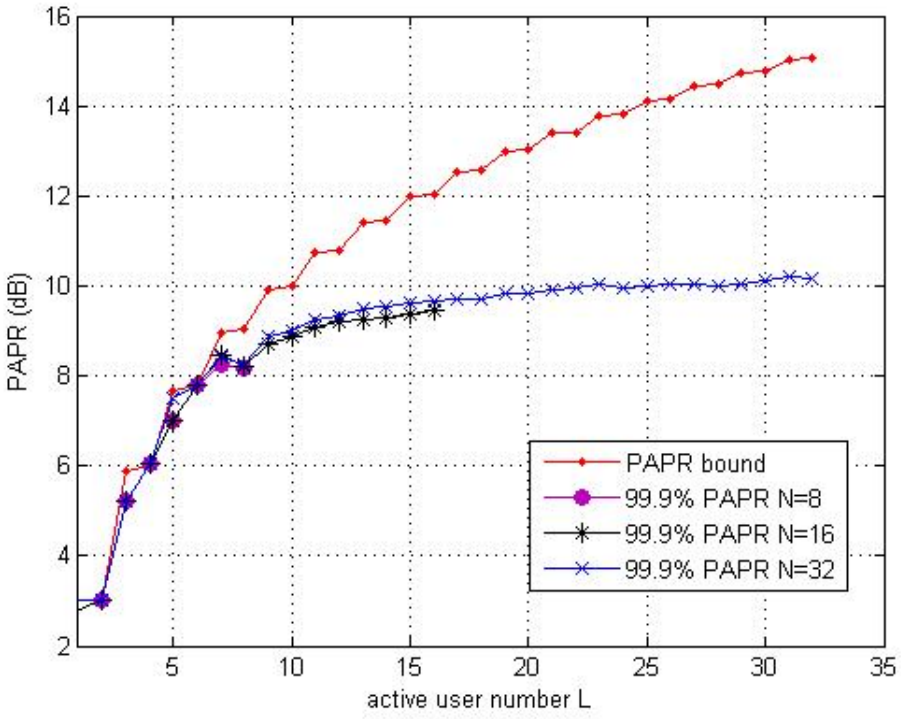

Figure 6.1: PAPR theoretical bound and 99.9% PAPRs of uncoded QPSK MC-CDMA (K=1)

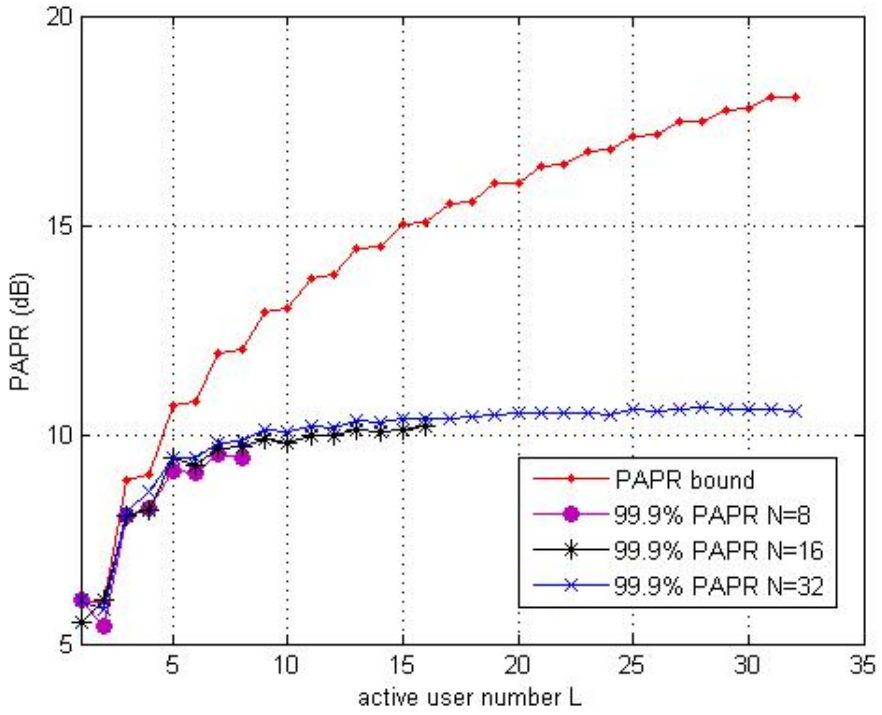

Figure 6.2: PAPR theoretical bound and 99.9% PAPRs of uncoded QPSK MC-CDMA (K=2)

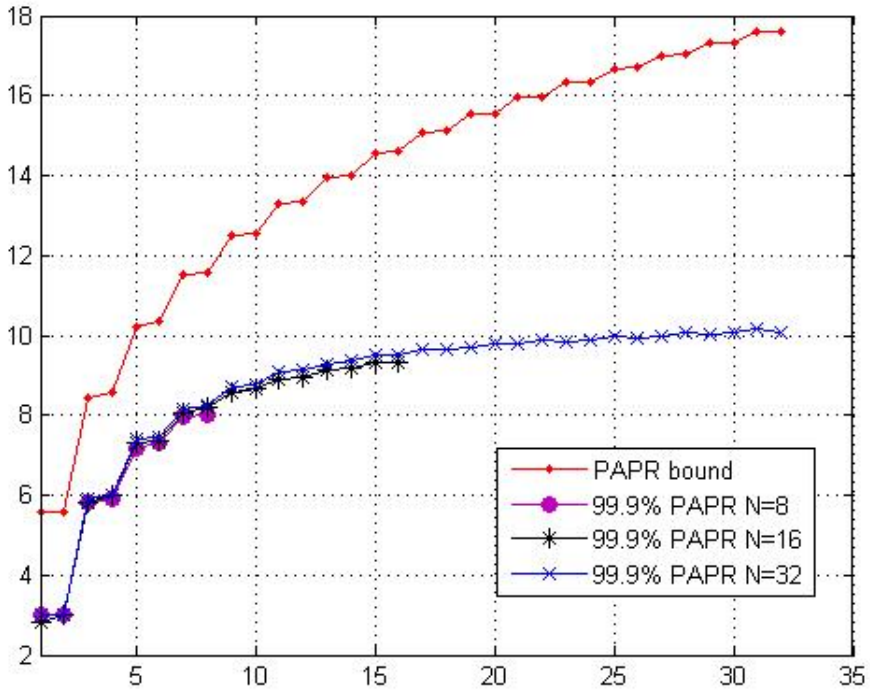

Figure 6.3: PAPR theoretical bound and 99.9% PAPRs of uncoded 16-QAM MC-CDMA (K=1)

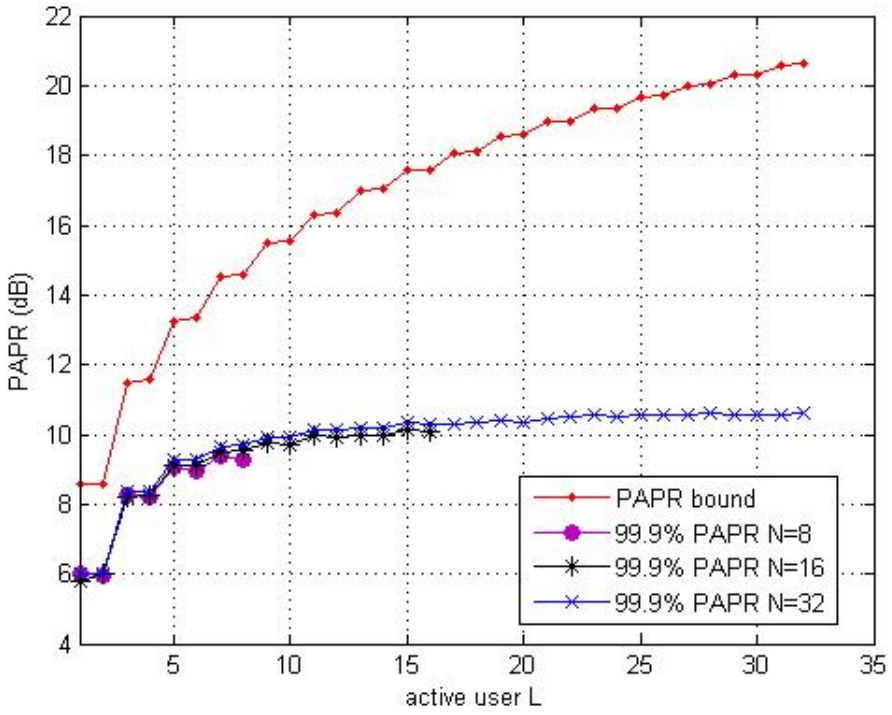

Figure 6.4: PAPR theoretical bound and 99.9% PAPRs of uncoded 16-QAM MC-CDMA (K=2)

OFDM symbol, whereas each user transmits QPSK Golay sequences of length $K = 4,\ 8$ and 16 in coded case. It is clear that the 99.9% PAPRs of uncoded and coded cases well follow the theoretical PAPR bound. In addition, the 99.9% PAPRs of uncoded and coded cases are almost identical. The results demonstrate that for various K of coded cases, their 99.9% PAPRs are almost identical to that of the uncoded case with $K = 2$, where QPSK modulation is employed. As predicted by their theoretical bounds, the PAPR of coded case has no dependency on the number of K, which implies that the coding scheme equivalently reduces the PAPR for large K.

Figure 6.9 shows the PAPR bound and 99.9% PAPRs of coded MC-CDMA with $N = 16$. In coded MC-CDMA of this figure, each user transmits 16-QAM ($\mathcal{A}$) Golay sequences of length $K = 4, 8$ and 16 respectively. From this figure, we can find that the coded 99.9% PAPRs well follow the theoretical PAPR bound. At the same time, their 99.9% PAPRs of various K are of no big differences. It demonstrated that 16-QAM ($\mathcal{A}$) Golay sequences coded MC-CDMA has no dependency on the spreading process K.

Figure 6.10 shows the 99.9% PAPRs of uncoded and coded MC-CDMA with $N = 16$. In uncoded MC-CDMA of Figure 6.10, each user transmits two 16-QAM modulated symbols in an OFDM symbol. In coded MC-CDMA of this figure, each user transmits 16-QAM ($\mathcal{B}$) Golay sequences of length $K = 4, 8$ and 16 respectively. In Figure 6.10, for various K of coded cases, their 99.9% PAPRs are

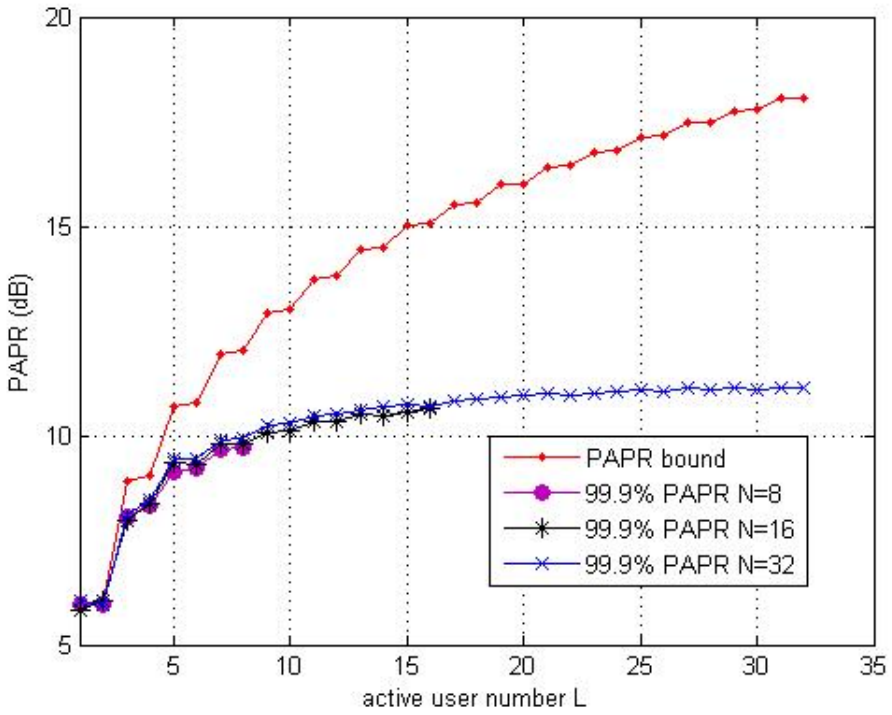

Figure 6.5: PAPR theoretical bound and 99.9% PAPRs of QPSK Golay sequences coded MC-CDMA (K=16)

almost identical to that of the uncoded case with $K = 2$. Consequently, Figure 6.10 numerically confirmed that the PAPR of coded case has no dependency on the number of K.

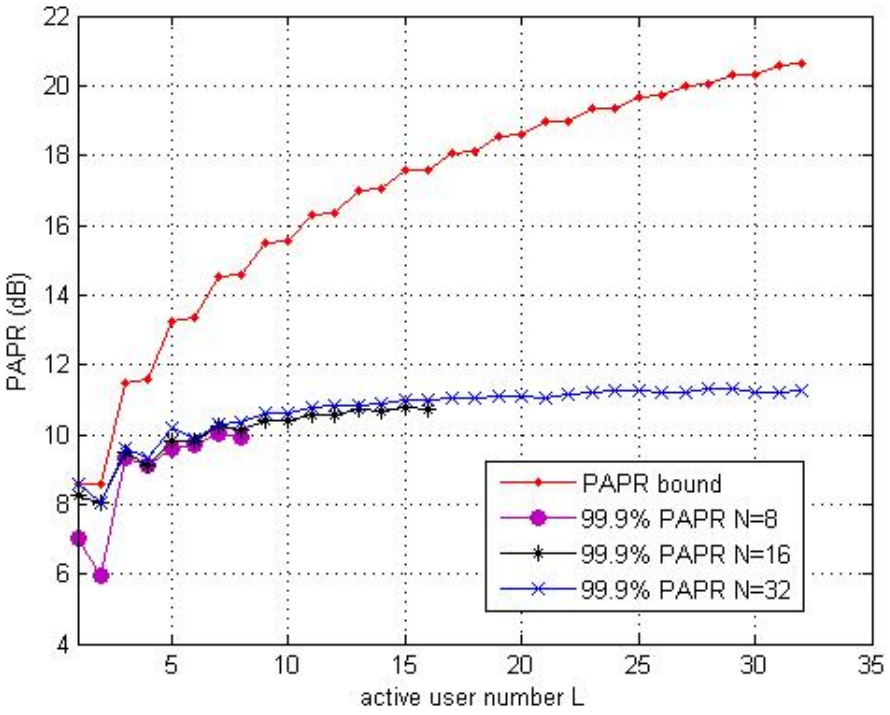

Figure 6.6: PAPR theoretical bound and 99.9% PAPRs of 16-QAM ($\mathcal{A}$) Golay sequences coded MC-CDMA (K=16)

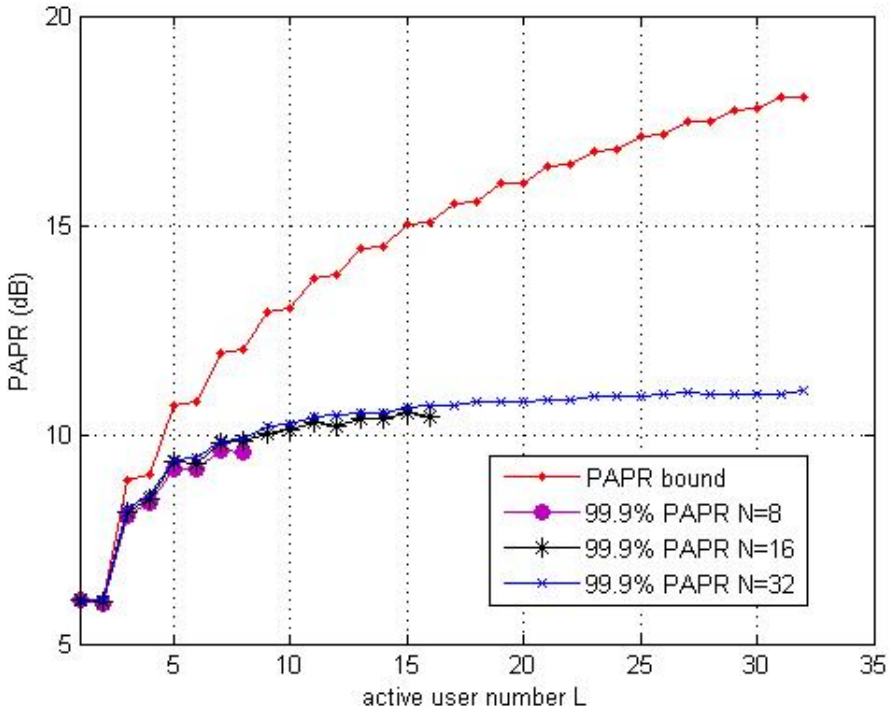

Figure 6.7: PAPR theoretical bound and 99.9% PAPRs of 16-QAM ($\mathcal{B}$) Golay sequences coded MC-CDMA (K=16)

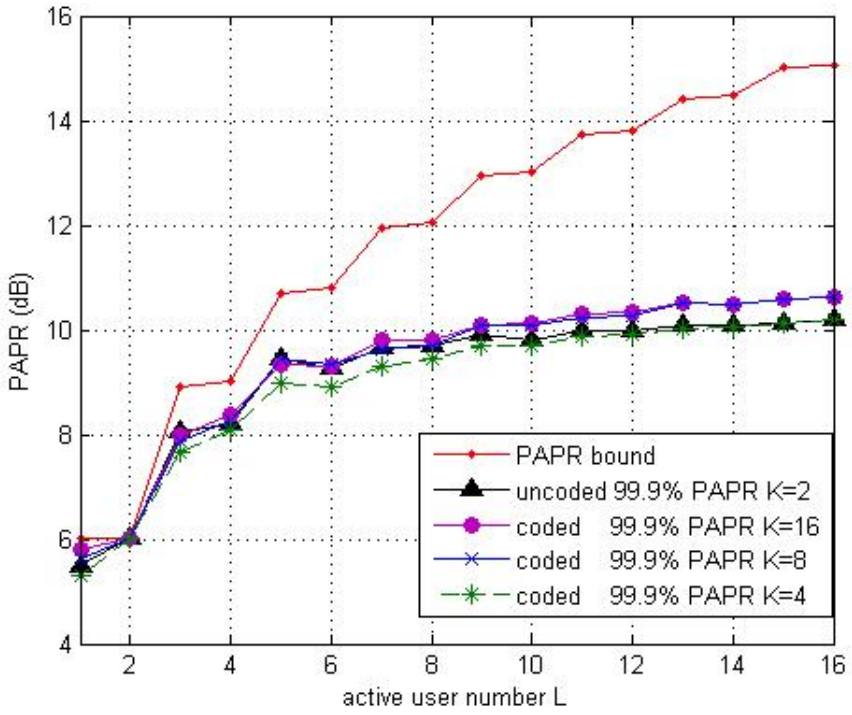

Figure 6.8: PAPR theoretical bound and 99.9% PAPRs of uncoded QPSK and QPSK Golay sequences coded MC-CDMA (N=16)

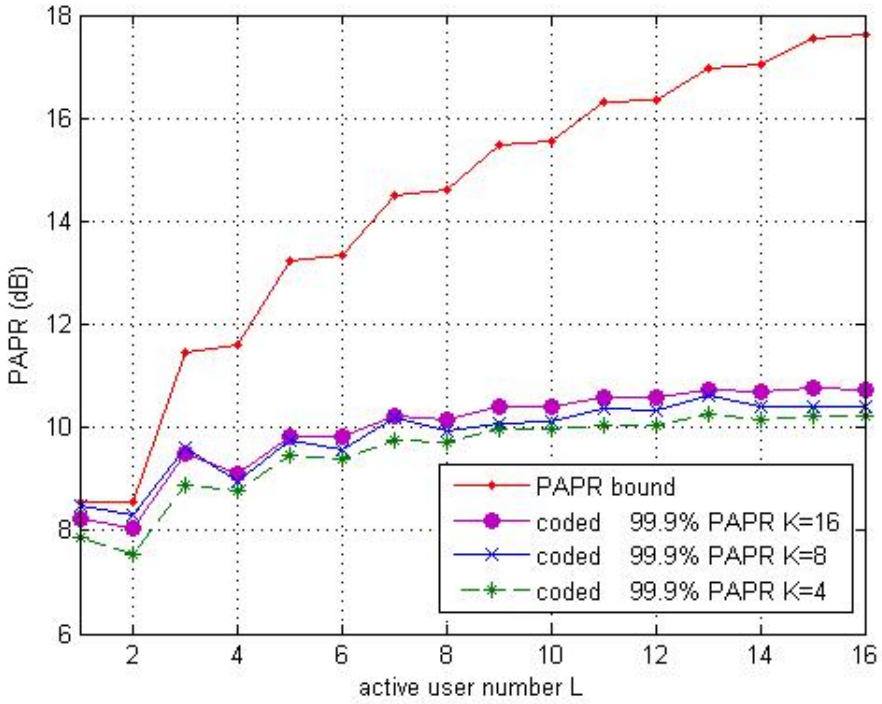

Figure 6.9: PAPR theoretical bound and 99.9% PAPRs of uncoded 16-QAM and 16-QAM ($\mathcal{A}$) Golay sequences coded MC-CDMA (N=16)

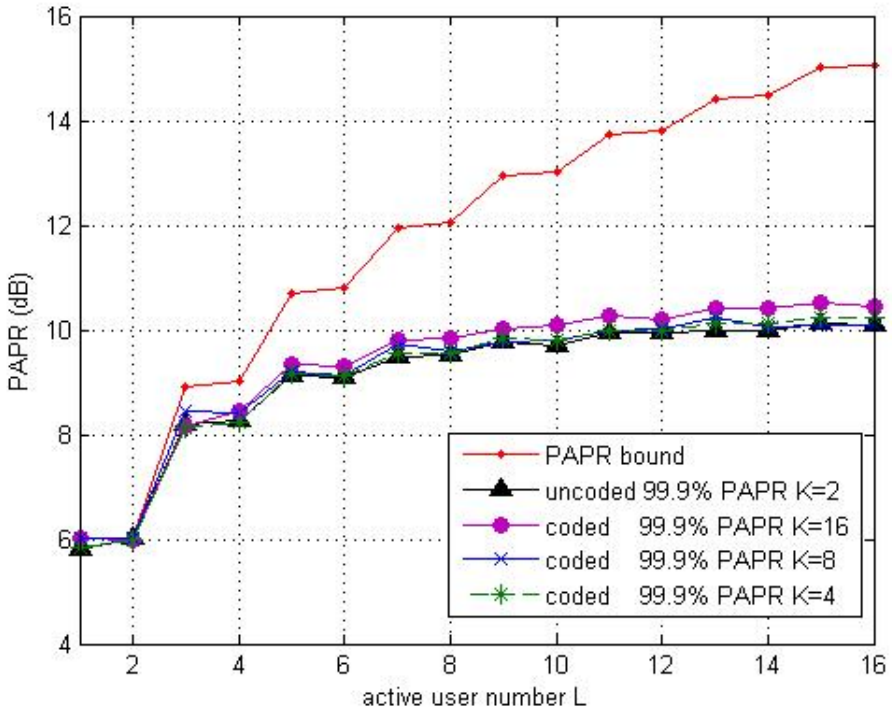

Figure 6.10: PAPR theoretical bound and 99.9% PAPRs of uncoded 16-QAM and 16-QAM Golay ($\mathcal{B}$) coded MC-CDMA (N=16)

Chapter 7

Conclusions

In this thesis, we presented theoretical PAPR bounds of uncoded and coded downlink MC-CDMA systems by employing Golay complementary sequences for spreading and/or coding. The simulation results numerically demonstrate our theoretical PAPR bounds. We found from the simulation results that the 99.9% PAPRs of uncoded and coded MC-CDMA well follow their theoretical trends, respectively. For the uncoded case, the PAPR depends on the number of active users L and the number of spreading processes K. For the coded case, the PAPR depends on the number of active users L only. Compared to the uncoded cases, coded cases effectively reduce the PAPR of downlink MC-CDMA system as predicted in theoretical analysis. In this way, we can achieve low PAPR of coded MC-CDMA system with a large number of subcarriers at the cost of code rate loss. However, as Figures 6.1, 6.2, 6.3, 6.4, 6.5, 6.6 and

6.7 show, when the active user number L increases, our theoretical PAPR bounds are not tight enough to keep track of the numerical 99.9% PAPRs in both uncoded and coded cases. We will focus on developing tighter bounds in our further researches.

Bibliography

[1] N. Yee, J.-P. Linnartz and G. Fettweis, "Multicarrier CDMA in indoor wireless radio networks," *Proc. of IEEE PIMRC*, pp. 109-113, Sep. 1993.

[2] A. Chouly, A. Brajal and S. Jourdan, "Orthogonal multicarrier techniques applied to direct sequence spread spectrum CDMA systems," *Proc. of IEEE GLOBECOM*, pp. 1723-1728, Nov. 1993.

[3] G. Fettweis, A. Bahai, and K. Anvari, "On multi-carrier code division multiple access (MC-CDMA) modem design" *Proc. of IEEE VTC' 94*, pp. 1670-1674, June 1994.

[4] S. Litsyn, *Peak Power Control in Multicarrier Communications*, Cambridge University Press, 2007.

[5] J. Jedwab, "Comment: M-sequences for OFDM peak-to-average power ratio reduction and error correction," *Electronic Letters*, vol. 33, pp. 1293-1294, Jul. 1997.

[6] I. Kalet, "The multitone channel," *IEEE Trans. Commun.*, vol. 37, pp. 119-124, Feb. 1989.

[7] S. H. Han and J. H. Lee, "An overview of peak-to-average power ratio reduction techniques for multicarrier transmission", *IEEE Wireless Commun.*, vol. 12, pp. 56-65, Apr. 2005.

[8] S. Nobilet, J. F. Hélard, D. Mottier, "Spreading sequences for uplink and downlink MC-CDMA systems: PAPR and MAI minimization ", *European Transactions on Telecommunications*, vol. 13, no. 5, pp. 465–474, Sep. 2002.

[9] S. Jitapunkul, K. Wutthipornpong, J. Songthanasak and S. Kunaruttanapruk, "Peak to average power ratio reduction in MC-CDMA using partial transmit sequences", *Wireless Telecommunications Symposium*, pp. 3, Aug. 2004.

[10] M. Sabbaghian and D. Falconer, "Peak to average power ratio properties of MC-CDMA and SM-CDMA", *IEEE 63rd VTC*, vol. 4, pp. 2013, Sept. 2006.

[11] L. Yang and E. Alsusa, "Dynamic code-allocation based PAPR reduction technique for MC-CDMA systems", *IEEE Wireless Communications and Networking Conference*, pp. 627, Jun. 2007.

[12] L. A. P. Hernandez and M. G. Otero, "User reservation approach for peak-to-average power ratio reduction in MC-CDMA systems", *IEEE 69th VTC*, pp. 1, Jun. 2009.

[13] R. manjith, S. C. Ramesh and M. M. I. Majeed, "Papr reduction in OFDM & MC-CDMA system using nonlinear companding techniques", *IEEE Region 8 International Conference on Computational Technologies in Electrical and Electronics Engineering (SIBIRCON)*, pp. 274, Aug. 2010.

[14] B. M. Popović, "Spreading sequences for multi-carrier CDMA systems", *IEE Colloquium on CDMA Techniques and Applications for Third Generation Mobile Systems*, pp. 8/1-8/6, May, 1997.

[15] H. Ochiai and H. Imai, "OFDM-CDMA with peak power reduction based on the spreading sequences", *IEEE ICC*, vol.3, pp. 1299-1303, Jun. 1998.

[16] K. Kang, K. Choi and S. K. Shin, "Reduced search for optimum code sets to reduce PAPR in MC-CDMA system", *The 5th International Symposium on Wireless Personal Multimedia Communications*, vol.1, pp. 135-139, Oct. 2002.

[17] H. Hubner, "Analog and digital multiplexing by means of Walsh functions", *Proc. Symp. Applications of Walsh Functions*, Washington, pp. 238-247, 1970.

[18] R. Gold, "Optimal binary sequences for spread spectrum multiplexing", *IEEE Trans. Inf. Theory*, vol. IT-13, pp. 619-621, 1967.

[19] J. Zhu, X. Wu, "A spread spectrum modulation method of forward CDMA channel in cellular system", *5th IEEE International Symposium on Wireless Networks*, vol. 4, pp. 1335, Sep. 1994.

[20] D. C. Chu, "Polyphase codes with good periodic correlation properties", *IEEE Trans. Inf. Theory*, vol. IT-18, pp. 531-532, Jul. 1972.

[21] A. B. Boehmer, "Binary pulse compression codes," *IEEE Trans. Inf. Theory*, vol. IT-13, pp. 156-167, Apr. 1967.

[22] M. Golay, "Complementary series," *IRE Trans. Inf. Theory*, vol. IT-7, pp. 82-87, 1961.

[23] J. A. Davis and J. Jedwab, "Peak-to-mean power control for OFDM, Golay complementary sequences, and Reed-Muller codes", *IEEE Trans. Inf. Theory*, vol. 45, no. 7, pp. 2397-2417, Nov. 1999.

[24] C. Rößing, V. Tarokh, "A construction of OFDM 16-QAM sequences having low peak powers," *IEEE Trans. Inf. Theory*, vol. 47, pp. 2091–2094, Nov. 2001.

[25] C. V. Chong, R. Venkataramani and V. Tarokh, "A new construction of 16-QAM Golay complementary sequences," *IEEE Trans. Inf. Theory*, vol. 50, pp.1374 - 1374, June 2004.

[26] R. Chang and R. Gibby, "A theoretical study of performance of an othogonal multiplexing data transmission scheme," *IEEE Trans. Commun. Technol.*, vol. 16, pp. 529-540, Aug. 1968.

[27] S. Weinstein and P. Ebert, "Data transmission by frequency-division multiplexing using the discrete fourier transform," *IEEE Trans. Commun. Technol.*, vol. 19, pp. 628-634, Oct. 1971.

[28] A. Peled and A. Ruiz, "Frequency domain data transmission using reduced computational complexity algorithms," *IEEE International Conference on Acoustics, Speech, and Signal Processing*, pp. 964-967, Apr. 1980.

[29] B. Hirosaki, "An orthogonally multiplexed QAM system using the discrete fourier transform," *IEEE Trans. Commun.*, vol. 29, pp. 982-989, Jul. 1981.

[30] ETSI (1997) *Digital Audio Broadcasting (DAB); Distribution interfaces; Ensemble Transport Interface (ETI) (ETS 300 799)*, June 1997.

[31] ETSI (1997) *Digital Video Broadcasting (DVB); Implementation of Binary Phase Shift Keying (BPSK) modulation in DVB satellite transmission systems (TR 101 198)*, Sept. 1997.

[32] IEEE Std., *Part 11: Wireless LAN medium access control (MAC) and physical layer (PHY) specifications*, IEEE stardard 802.11-2007 ed., 2007.

[33] IEEE Std., *Part 11: Wireless LAN medium access control (MAC) and physical layer (PHY) specifications, Amendment 5: enhancements for higher throughput*, IEEE standard 802.11n-2009 ed., 2009.

[34] T. Pollet, M. van Bladel, and M. Moeneclaey, "BER sensitivity of OFDM systems to carrier frequency offset and wiener phase noise," *IEEE Trans. Commun.*, vol. 43, pp. 191-193, Aug. 2002.

[35] H. Sari, G. Karam, and I. Jeanclaude, "Transmission techniques for digital terrestrial TV broadcasting," *IEEE Commun. Mag.*, pp. 100-109, Feb. 1995.

[36] J. G. Proakis and M. Salehi, *Digital Communications*, 5th ed, McGraw-Hill, Inc., 2008.

[37] R. A. Scholtz, "The origins of spread-spectrum communications," *IEEE Trans. Commun.*, vol. 5, pp. 822-854, May 1982.

[38] R. L. Pickholtz, D. L. Schilling and L. B. Milstein, "Theory of spread-spectrum communications—a tutorial," *IEEE Trans. commun.*, vol. 30, pp. 855-884, May 1982.

[39] O. C. Yue, "Spread spectrum mobile radio," *IEEE Trans. Veh. Technol.*, vol. 32, pp. 98-105, Feb. 1983.

[40] M. Simon, J. Omura, R. Scholtz and B. Levitt, *Spread Spectrum Communications Handbook*, New York, USA: McGraw-Hill, 1994.

[41] IEEE Std., *Part 15.4: Wireless Medium Access Control (MAC) and Physical Layer (PHY) Specifications for Low-Rate Wireless Personal Area Networks (WPANs)*, IEEE standard 802.15.4-2006 ed., 2006.

[42] K. Gillhousen, I. Jacobs, R. Padovani, A. Viterbi, L. Weaver Jr., and C. Wheatley III, "On the capacity of a cellular CDMA system," *IEEE Trans. on Veh. Technol.*, vol. 40, pp. 303-312, May 1991.

[43] L. Hanzo, M. Münster, B.-J. Choi, and T. Keller, *OFDM and MC-CDMA for Broadband Multi-user Communications*, WLANs and Broadcasting, John Wiley & Sons, 2003.

[44] A. J. Viterbi, *CDMA: Principles of Spread Spectrum Spectrum Communication*, Addison-Wesley Publishing Company, 1995.

[45] N. Yee and J.P. Linnartz, "MICRO 93-101: Multi-carrier CDMA in an indoor wireless radio channel," *Tech. Rep.*, 1994.

[46] S. Kaiser, "MC-FDMA and MC-TDMA versus MC-CDMA and SS-MC-MA: performance evaluation for fading channels," *IEEE 5th International symposium on Spread Spectrum Techniques and Applications*, pp. 200-204, Sept. 1998.

[47] J. P. Berens, F. Blanz, J. Plechinger and J. Res, "Performance of multicarrier joint detection CDMA mobile communications systems," *IEEE 47th VTC*, vol. 3, pp. 1892, May 1997.

[48] S. Nahm and W. Sung, "Time- and frequency- domain hybrid detection scheme for OFDM-CDMA systems," *IEEE ICC*, vol. 3, pp. 1531, Jun. 1998.

[49] S. Narahashi and T. Nojima, "New phasing sheme of N-multiple carriers for reducing peak-to-average power ratio," *Electronics Letters*, vol. 30, pp. 1382-1383, Aug. 1994.

[50] M. Friese, "Multicarrier modulation with low peak-to-average power ratio," *Electronics Letters*, vol. 32, pp. 713-714, Apr. 1996.

[51] P. V. Eetvelt, G. Wade, and M. Tomlinson, "Peak to average power reduction for OFDM schemes by selective scrambling," *Electronics Letters*, vol. 32, pp, 1963-1964, Oct. 1996.

[52] M.R. Schroeder, "Synthesis of low-peak-factor signals and binary sequences with low autocorrelation," *IEEE Trans. Inf. Theory*, pp. 85-89, 1970.

[53] X. Li and J.A. Ritcey, "M-sequences for OFDM peak-to-average power ratio reduction and error correction," *Electronics Letters*, vol. 33, pp. 554-555, Mar. 1997.

[54] W. Rudin, "Some theorems on Fourier coefficients," *Proceedings of American Mathematics Society*, vol. 10, pp. 855-859, Dec. 1959.

[55] D. J. Newman, " An L^1 extrimal problem for polynomials," *Proceedings of American Mathematics Society*, vol. 16, pp. 1287-1290, Dec. 1965.

[56] B. M. Popovic, "Synthesis of power efficient multitone signals with flat amplitude spectrum," *IEEE Trans. Commun.*, vol. 39, no. 7, pp. 1031-1033, Aug. 2002.

[57] M. G. Parker, K. G. Paterson, and C. Tellambura, "Golay complementary sequences", *Wiley Encyclopedia of Telecommunications*, Edited by J.G. Proakis, Wiley Interscience, 2002.

[58] D. Wulich and L. Goldfeld, "Reduction of peak factor in orthogonal multicarrier modulation by amplitude limiting and coding," *IEEE Trans. Commun.*, vol. 47, no. 1, pp. 18-21, Jan. 1999.